EUKARYOTIC CELL, Jan. 2010, p. 22–30 Vol. 9, No. 1
1535-9778/10/$12.00 doi:10.1128/EC.00196-09

Leishmania major MPK7 Protein Kinase Activity Inhibits Intracellular Growth of the Pathogenic Amastigote Stage[▽]

Miguel A. Morales, Pascale Pescher, and Gerald F. Späth*

Institut Pasteur, CNRS URA 2581, Laboratory of Parasite Virulence, and the Institut National de la Santé et de la Recherche Médicale (INSERM) Avenir Program, 75015 Paris, France

Received 2 July 2009/Accepted 22 September 2009

During the infectious cycle, protozoan parasites of the genus *Leishmania* undergo several adaptive differentiation steps that are induced by environmental factors and crucial for parasite infectivity. Genetic analyses of signaling proteins underlying *Leishmania* stage differentiation are often rendered difficult due to lethal null mutant phenotypes. Here we used a transgenic strategy to gain insight into the functions of the mitogen-activated *Leishmania major* protein kinases LmaMPK7 and LmaMPK10 in parasite virulence. We established *L. major* and *Leishmania donovani* lines expressing episomal green fluorescent protein (GFP)-LmaMPK7 and GFP-LmaMPK10 fusion proteins. The transgenic lines were normal in promastigote morphology, growth, and the ability to differentiate into metacyclic and amastigote stages. While parasites expressing GFP-LmaMPK10 showed normal infectivity by mouse footpad analysis and macrophage infection assays, GFP-LmaMPK7 transgenic parasites displayed a strong delay in lesion formation and reduced intracellular parasite growth. Significantly, the effects of GFP-LmaMPK7 on virulence and proliferation were due exclusively to protein kinase activity, as the overexpression of two kinase-dead mutants had no effect on parasite infectivity. GFP-LmaMPK7 transgenic *L. donovani* cells revealed a reversible, stage-specific growth defect in axenic amastigotes that was independent of cell death but linked to nonsynchronous growth arrest and a significant reduction of de novo protein biosynthesis. Our data suggest that LmaMPK7 protein kinase activity may be implicated in parasite growth control and thus relevant for the development of nonproliferating stages during the infectious cycle.

Leishmaniasis is an important neglected infectious disease that represents a major global health problem affecting more than 12 million people worldwide (12). The disease is caused by pathogenic protozoa of the genus *Leishmania*, which generate a variety of pathologies ranging from self-healing cutaneous lesions to fatal visceral involvement and hepatosplenomegaly (3). During the infectious cycle, *Leishmania* differentiates from the extracellular promastigote form that develops in the midgut of the sand fly host to the intracellular amastigote form that differentiates and multiplies inside the macrophage phagolysosome of the mammalian host. These developmental transitions are triggered by environmental factors, i.e., the pH and temperature encountered in insect and mammalian hosts (47). The relevance of environmental sensing in *Leishmania* biology is highlighted by the evolutionary expansion of members of the STE and CMGC (cyclin-dependent kinase [CDK], mitogen-activated protein kinase [MAPK], glycogen synthase kinase 3 [GSK3], and CLK) protein kinase families, which are implicated in extracellular-regulated signal transduction through the activation of MAPKs (27). The *Leishmania* genome encodes MAPKs and MAPK-like kinases (27), some of which were previously genetically implicated in parasite virulence and flagellar biogenesis (reviewed in references 29 and 44). The genetic analysis of other *Leishmania* MAPKs is rendered difficult by lethal null mutant phenotypes. For example, null mutants of *Leishmania mexicana* LmxMPK4 and the *L. major* protein LmaMPK7 (the subject of this study) can be generated only in the presence of the respective transgene, indicating that these kinases are essential for promastigote growth in vitro (42; M. A. Morales, R. Watanabe, and G. F. Späth, unpublished data). One possible strategy to overcome this limitation and gain insight into the functions of these essential protein kinases is provided by the biochemical characterization of epitope-tagged derivatives expressed in transgenic parasites. We previously utilized recombinant *Leishmania* MAPKs to study protein kinase activities (22). The expression of three green fluorescent protein (GFP)-tagged *Leishmania major* MAPKs, LmaMPK4, LmaMPK7, and LmaMPK10, allowed us to reveal environmentally and developmentally regulated phosphorylation and induction of phosphotransferase activity of these protein kinases after exposure to pH 5.5 and 34°C in transgenic *L. major* and in transgenic *Leishmania donovani* axenic amastigotes. In addition, we identified LmaMPK10 independently as being an amastigote-specific phosphoprotein by using a proteomics approach (23). Together, these data indicate a functional conservation of *Leishmania* MAPKs in parasite environmental sensing and link this pathway to amastigote differentiation.

The transduction of extracellular signals through MAPKs modulates many important functions across all eukaryotes, including cytokine-dependent immune regulation and growth factor-induced ontogenesis in higher vertebrates, mating-type switching in yeast, and the expression of stage-specific virulence determinants in pathogenic microbes (18). These MAPK functions are executed through the phosphorylation of a wide range of substrates, which are involved in growth control and differential gene expression. Mammalian MAPKs control cell

* Corresponding author. Mailing address: Institut Pasteur, 25 rue du Dr. Roux, 75015 Paris, France. Phone: 33.1.40.61.38.58. Fax: 33.1.45.68.83.32. E-mail: gerald.spaeth@pasteur.fr.

▽ Published ahead of print on 2 October 2009.

cycle progression by activating cyclin D1-cdk4 or cyclin B-CDC2 complexes (4, 46) and are involved in mechanisms of posttranscriptional regulation, including mRNA processing, modifications of mRNA stability, and the control of translation initiation (2, 9, 28). MAPKs regulate transcription and control differential gene expression through nuclear factors (8), which are recognized as substrates and translocate to the nucleus following phosphorylation, where they modulate gene expression through binding to *cis*-regulatory sequence elements. *Leishmania* differential gene expression substantially differs from this paradigm. The absence of transcription factors from the parasite genome (19) raises important questions regarding the nature of *Leishmania* MAPK substrates, which may be implicated in parasite-specific mechanisms of gene expression, such as polycistronic transcription and *trans*-splicing (6), or mechanisms of posttranscriptional and posttranslational regulation (5).

Here we show that the transgenic expression of active LmaMPK7, but not inactive kinase, leads to a significant attenuation of parasite virulence, which was due to a reversible, nonsynchronous growth arrest specific to the intracellular amastigote stage. Our data thus establish a first link of LmaMPK7 to *Leishmania* growth control, with potential relevance for the development of nonproliferative stages during the infectious cycle.

MATERIALS AND METHODS

Parasites. *Leishmania major* strain Friedlin V1 (MHOM/JL/80/Friedlin) was grown in M199 medium at 26°C (21). *L. donovani* strain 1S2D (MHOM/SD/62/1S-CL2D) clone LdB was cultured as described previously (10, 15, 17, 30). *L. major* and *L. donovani* pXG mock-transfected control and GFPK transgenic parasites expressing GFP-tagged LmaMPKs and inactive dead mutant kinase were generated as previously described (22). To control for nonspecific effects associated with the GFP tag, transgenic *L. donovani* lines expressing pLEXSY-LmaMPK7 or vector alone were established. The transgenic parasites were cultured in M199 medium supplemented with 100 μg/ml G418 (for pXG) and 75 μg/ml hygromycin B (for pLEXSY). Cured GFPK lines with reduced episome copy numbers were established by growing the parasites for 15 passages in G418-free medium. We routinely passage all parasite lines through mice before performing virulence tests in order to eliminate nonspecific effects due to a loss of virulence during prolonged in vitro culture.

Metacyclic purification. (i) Agglutination. Metacyclic parasites were isolated from 5-day stationary parasites by agglutination (7). Briefly, 1×10^8 to 2×10^8 cells/ml were incubated for 30 min at room temperature (RT) with 50 μg/ml peanut agglutinin in M199 medium without serum, agglutinated parasites were removed by centrifugation for 10 min at $200 \times g$, and metacyclic parasites were recovered from the supernatant by centrifugation for 15 min at $1{,}990 \times g$. Parasite fractions were washed once in 10 ml M199 medium by centrifugation.

(ii) Ficoll gradient enrichment. Parasites were purified as described previously (34). Briefly, a 20% stock solution of Ficoll type 400 (Sigma, St. Louis, MO) was prepared in sterile, endotoxin-free water filtered through a 0.22-mm cellulose acetate filter and kept at 4°C in darkness for no longer than 1 month. Working dilutions were prepared on the day that they were used. We used 15-ml Falcon conical centrifuge tubes containing 2 ml of 10% Ficoll at the bottom, overlaid by 2 ml of stationary-phase parasites (2×10^8cells/ml) suspended in M199 medium. These step gradients were centrifuged for 10 min at $1{,}300 \times g$ at room temperature, and the parasites were recovered from the interface with a sterile Pasteur pipette. Parasite fractions were washed once in 10 ml M199 medium by centrifugation.

Mouse strains and infections. BALB/c mice were obtained from Charles River Breeding Laboratories. C57BL/6-*Cybb*^{tm1} null mutant (*phox*$^-$) mice were obtained from the Jackson Laboratory. Parasite virulence was assessed by footpad analysis as described previously (40). Groups of five BALB/c mice were injected subcutaneously with 3×10^5 metacyclic parasites prepared by Ficoll density gradient centrifugation (see above) in the left hind footpad (38). We monitored lesion development by measuring the thickness of the footpad with a Vernier caliper. Lesion parasites were enumerated by limiting-dilution assay (39).

Macrophage infections. Peritoneal exudate macrophages (PEMs) were seeded in 24-well plates onto glass coverslips and incubated the following day in Dulbecco's modified Eagle's medium (DMEM)–0.7% bovine serum albumin (BSA) for 2 h at 34°C with 10^5 purified metacyclic parasites. Free parasites were removed by washing, and cultures were further incubated at 34°C in a CO_2 incubator until the end of the experiment. Infection efficiency and intracellular parasite burden were determined by nuclear staining and fluorescence microscopy as described previously (36).

Complement lysis. Human serum was obtained from healthy volunteers. After incubation of blood to allow clotting for 10 min at RT, serum was recovered by centrifugation for 10 min at $6{,}000 \times g$ at 4°C. A total of 10^6 promastigotes from logarithmic-phase cultured cells were incubated with human serum in 500 μl DMEM containing 40 μg/ml propidium iodide for 30 min at RT, and lysis was determined by flow cytometry as described previously (36).

Proliferation assay. Log-phase parasites were washed twice in phosphate-buffered saline (PBS) and resuspended in 1 ml M199 medium without serum to obtain a final concentration of 10^5 parasites/ml, and carboxyfluorescein diacetate succinimidyl ester (CFSE) (Molecular Probes) was added to a final concentration of 5 μM. Cells were incubated at 26°C for 10 min and gently mixed 3 to 4 times, 2 volumes of medium M199 medium was added, and after centrifugation at $1{,}200 \times g$ for 5 min, stained cells were resuspended in fresh medium supplemented with 20% heat-inactivated calf serum and further cultivated in 25-cm^2 tissue culture flasks at 37°C in the presence of 100 μg/ml G418. CFSE fluorescence was determined at 2 h and 72 h after staining by flow cytometry using the Becton Dickinson FACSCalibur system.

Cell cycle analysis. Parasites were fixed overnight with 70% ethanol–5% glycerol at −20°C, washed once in PBS, and incubated with 15 μg/ml RNase for 15 min at 37°C. Parasites were thereafter incubated with 10 μg/ml propidium iodide (Sigma) for 1 h at 26°C. The nuclear DNA content of transfectant and control cells was analyzed with a FACSCalibur flow cytometer. Cells with the DNA content 2n/4n were gated on a fluorescence pulse-versus-area measurement to exclude cell doublets from the analysis. The percentage of cells in different cell cycle phases was calculated by using the Watson pragmatic model of FlowJo (v6.1) software (Tree Star, Inc., San Carlos, CA).

Immunofluorescence analysis. Infected PEMs established on glass coverslips were washed once in PBS, fixed by incubation in 3.5% paraformaldehyde for 5 min at RT, permeabilized with 100% ethanol at 4°C for 15 min, and rehydrated for 10 min at RT in PBS. Cells were incubated sequentially for 20 min at 37°C with 1:500-diluted WIC79.3 (36) and 1:100-diluted Texas Red-conjugated anti-mouse secondary antibody (Molecular Probes). Nuclear counterstaining was performed with 0.5 μg/ml Hoechst 33342 dye in PBS.

Metabolic labeling. A total of 6×10^7 *L. donovani* cells were resuspended in 1 ml of labeling medium (DMEM without Cys and Met) at 4°C, and 400 μCi of Pro-Mix containing L-[^{35}S]methionine and L-[^{35}S]cysteine (GE Healthcare) was added. The cells were incubated for 2 h and washed three times with M199 medium. Proteins from equal numbers of pro- and amastigotes at different time points were lysed, precipitated with trichloroacetic acid, and dried onto glass microfiber filters (Whatman, England). Label incorporation was measured with a scintillation counter.

Protein extraction and Western blot analysis. *L. donovani* axenic amastigotes were harvested from cultures at a density of 8×10^6 cells/ml, transferred into prechilled Falcon tubes, and centrifuged for 10 min at 4°C and $700 \times g$. Supernatants were removed, and cells were washed twice in RPMI 1640 medium. Cell pellets were resuspended in 1 ml lysis buffer containing 150 mM NaCl, 1% Triton X-100, 50 mM Tris-HCl, 0.25% CHAPS {3-[(3-cholamidopropyl)-dimethylammonio]-1-propanesulfonate}, 1% benzonase, and protease inhibitor cocktail (Roche). Samples were incubated for 30 min at 4°C and vortexed every 10 min. Following the removal of cellular debris by centrifugation, total protein extracts were quantified by using the Coomassie (Bradford) protein assay kit (Pierce). For phosphoprotein purification, the protein concentration was adjusted to 0.1 mg/ml, and 2.5-mg extracts were applied onto equilibrated affinity columns of a phosphoprotein purification kit (Qiagen) according to the manufacturer's instructions. Unbound proteins were removed by washing, and bound phosphorylated proteins were eluted in 1 ml elution buffer. Total protein extracts or purified phosphoproteins were separated on 4 to 12% Bis-Tris NuPAGE gels (Invitrogen) and blotted onto polyvinylidene difluoride (PVDF) membranes (Pierce). Proteins were revealed using the following antibodies: polyclonal anti-α subunit of eukaryotic initiation factor 2 (eIF2α) (kindly provided by D. Zilberstein, Technion, Israel) (S. Goline et al., unpublished data), mouse monoclonal anti-α-tubulin antibody (Sigma), and anti-chicken or anti-mouse horseradish peroxidase (HRP)-conjugated secondary antibodies (Invitrogen).

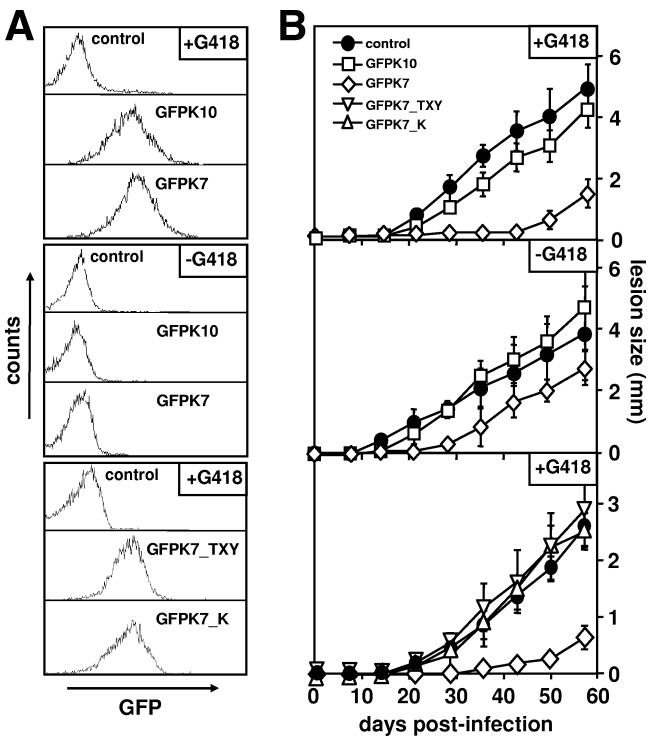

FIG. 1. Expression of active LmaMPK7 reduces *L. major* virulence. (A) FACS analysis. Promastigotes were cultured in the presence of 100 μg/ml G418 (+G418) (top and bottom) or maintained in culture for 15 passages without drug (−G418) (middle), and GFP fluorescence intensities in live cells were measured by flow cytometry. (B) Footpad analysis. A total of 3×10^5 metacyclic control parasites transfected with the vector alone (control) (●) and transgenic parasites expressing GFP-LmaMPK10 (GFPK10) (□), GFP-LmaMPK7 (GFPK7) (◇), and two GFP-LmaMPK7 kinase-dead mutants (GFPK7_TXY [▽] and GFPK7_K [△]) were inoculated into the hind footpad of female BALB/c mice, and lesion formation was monitored by measuring the increase in footpad size. Groups of five mice were analyzed, and standard deviations are indicated by bars. Two independent tests were performed, and data from one representative experiment are shown.

RESULTS

Transgenic expression of active LmaMPK7 in *L. major* leads to virulence attenuation. *L. major* and *L. donovani* transgenic parasites overexpressing GFP-tagged LmaMPK7 and LmaMPK10 (termed GFPK7 and GFPK10, respectively) allowed us in previous studies to reveal an increased activity of these kinases in response to heat and pH shock and following amastigote differentiation (22). Here we investigated the effects of LmaMPK overexpression on parasite virulence by using experimental mouse infection (35, 37).

Mock transfectants and GFPK lines were cultured in the presence of 100 μg/ml G418 to select for the robust expression of the GFP fusion proteins (Fig. 1A, top). Metacyclic parasites were isolated by agglutination (32), and groups of five BALB/c mice were inoculated with 3×10^5 GFPK7, GFPK10, and mock-transfected control parasites. The development of cutaneous lesions was monitored for several weeks postinfection by measuring footpad swelling with a Vernier caliper. Control parasites elicited a strong response 20 days after inoculation, which progressed steadily and ultimately resulted in necrotic lesions (Fig. 1B, top). In contrast, GFPK7 parasites were highly attenuated as judged by the delay in lesion formation, which was first detectable at day 50 postinfection and thus 30 days after the control. Attenuation was observed for several independent GFPK7 lines and correlated with reduced parasite burden, ruling out any nonspecific effects on virulence due to clonal variation (data not shown). Significantly, GFPK10 parasites showed normal infectivity, indicating that GFPK7 virulence attenuation is independent of nonspecific effects of either GFP or MAPK overexpression.

To further corroborate the link between LmaMPK7 expression and the attenuated phenotype, we established cured GFPK lines obtained by repeated parasite passage in medium without G418. After 15 in vitro passages, the cured lines showed a 38-fold reduction of episome copy numbers, as assessed by bacterial plating assays (data not shown), and a decline of GFP-LmaMPK fluorescence intensities to levels similar to those of the mock-transfected control (Fig. 1A, middle). The virulence of cured GFPK7 parasites was restored to levels approaching that of the control (Fig. 1B, middle), and both kinetics and the sizes of lesion formations were enhanced compared to those of the G418-selected line. As expected, the cure had no significant effect on virulent mock control or GFPK10. Together, these data establish a specific link between amastigote infectivity and the level of LmaMPK7 expression.

We previously observed a robust increase in GFP-LmaMPK7 protein kinase activity in axenic amastigotes compared to log-phase promastigotes (22). Hence, GFPK7 virulence attenuation may be a direct result of increased phosphotransferase activity. We tested this hypothesis by establishing transgenic *L. major* cultures expressing kinase-dead versions of GFP-LmaMPK7 mutated in either the activation loop (T335A/Y337F, termed GFPK7_TXY) or the serine-threonine kinase motif (K150R, termed GFPK7_K) (Fig. 1A, bottom) (22). While GFPK7 showed the expected delay in lesion formation, both transgenic lines expressing the kinase-dead mutants showed a virulence profile identical to that of the virulent mock control (Fig. 1B, bottom). Thus, reduced GFPK7 infectivity is a direct consequence of LmaMPK7 protein kinase activity.

Phenotypic characterization of GFPK7. In the following section, we investigated the molecular mechanisms underlying the attenuated GFPK7 virulence phenotype. We first analyzed the ability of GFPK7 to generate infective metacyclic parasites during stationary growth. By utilizing the lectin ricin agglutinin, which binds to procyclic but not metacyclic surface lipophosphoglycan (LPG) (32), we identified similar numbers of GFPK7 and control metacyclic parasites in stationary culture (Fig. 2A, left), which provided the needle-shaped morphology characteristic of this stage of the parasite (Fig. 2A, right). Identical results were obtained by using Ficoll density centrifugation (34), which allows for LPG-independent metacyclic isolation and thus guards against possible effects of LmaMPK7 overexpression on LPG structure and ricin-dependent purification (data not shown).

The *Leishmania* surface glycocalyx was shown previously to confer resistance to cytolytic host activities, including serum complement and the phagocytic oxidative burst (36). We probed the integrity of the GFPK7 surface coat by incubation with human serum and measurement of complement-mediated

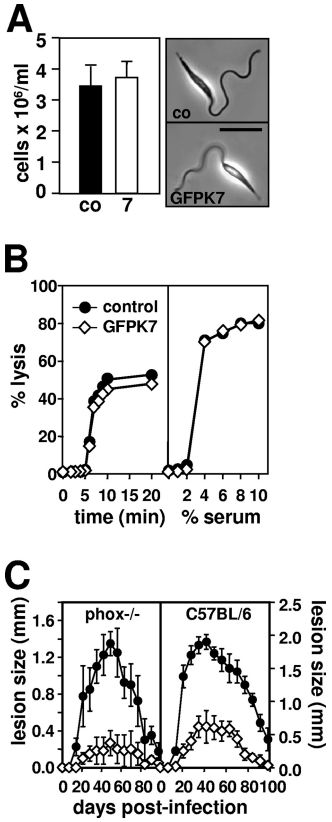

FIG. 2. *L. major* GFPK7 is normal in metacyclogenesis and resistance to cytotoxic host activities. (A) Agglutination assay. (Left) A total of 10^8 control (co) (black bar) and GFPK7 (7) (open bar) cells from 5-day stationary cultures were incubated with the lectin ricin agglutinin, and numbers of nonagglutinating metacyclic parasites were determined microscopically after differential centrifugation. Two independent experiments were performed, and data from one representative triplicate experiment, with standard deviations indicated by the bars, are shown. (Right) Phase-contrast images of control and GFPK7 metacyclic parasites prepared by ricin agglutination. The bar corresponds to 10 μm. (B) Complement lysis assay. GFPK7 (◇) and mock-transfected control (●) parasites from 5-day stationary cultures were incubated in the presence of 2% human serum (left) or increasing serum concentrations ranging from 0% to 10% (right), and cell lysis was monitored by propidium iodide incorporation and flow cytometry during a 20-min incubation period. Results represent average values obtained in one duplicate experiment. (C) Footpad analysis. A total of 5×10^5 metacyclic control (●) and GFPK7 (◇) parasites were inoculated into the left hind footpad of NADPH-oxidase-deficient *phox*$^{-/-}$ (left) and C57BL/6 control *phox*$^{+}$ (right) mice, and lesion development was determined by measuring footpad swelling with a Vernier caliper. The averages and standard deviations for groups of five mice are shown.

lysis by a fluorescence-activated cell sorter (FACS)-based approach (36). Both control and GFPK7 transgenic parasites were resistant to 2% serum (Fig. 2B, left) and showed a similar susceptibility to increasing concentrations, with complete lysis occurring at 10% serum levels (Fig. 2B, right). We next tested if GFPK7 is targeted by host oxidants following lesion development in infected C57BL/6 control and *phox*$^{-}$ mice. These mice lack the gp91 phox subunit of NADPH oxidase and, as a result, are unable to produce reactive oxidant species during the phagocytic oxidative burst (36). Similar to infections of susceptible BALB/c mice (Fig. 1B), GFPK7 transgenic parasites were highly attenuated in resistant C57BL/6 mice and elicited delayed and strongly reduced lesion formation (Fig. 2C, right). GFPK7 showed a similar infection profile in *phox*$^{-/-}$ mice (Fig. 2C, left), and hence, the virulence defect was not compensated for by the absence of oxidants. Together, these data demonstrate that GFPK7 virulence attenuation is independent of metacyclogenesis and cytotoxic complement or oxidants.

GFPK7 is attenuated in macrophage infection assays. We tested if GFPK7 virulence attenuation is due to a defect in amastigote differentiation. Peritoneal exudate macrophages (PEMs) were infected with purified metacyclic parasites of the mock control, GFPK7, and the kinase-inactive mutants GFPK7_TXY and GFPK7_K at a multiplicity of 10 parasites per host cell. Amastigote development was assessed by immunofluorescence analysis using LPG as a negative marker, which is not expressed at the intracellular stage (1). Two hours after infection, promastigote parasites were strongly decorated with the phosphoglycan-specific antibody WIC79.3 (41) due to the presence of surface LPG, which was also released into the host cell cytoplasm (Fig. 3A, top) (36). At 120 h after infection, control and GFPK7 parasites were no longer decorated with WIC79.3, suggesting a downregulation of LPG and normal amastigote differentiation (Fig. 3A, bottom).

Intracellular proliferation was monitored by nuclear staining and fluorescence microscopy. The number of intracellular parasites of the mock control and the transgenic lines expressing the kinase-dead mutants showed a fourfold increase over the infection period from initially 4 parasites per host cell at 2 h postinfection up to more than 16 parasites per host cell at day 5 (Fig. 3B), indicating robust intracellular proliferation. Although GFPK7 parasites colonized host cells at normal levels, with 4 parasites per infected host cell 2 h after infection, which subsequently differentiated into amastigotes (see above), these parasites showed a dramatic defect in intracellular growth as judged by the unchanged parasite burden throughout the infection period. We confirmed the GFPK7 growth defect in vivo by footpad infection. Female BALB/c mice were infected with metacyclic GFPK10 control and GFPK7 as described above, and parasite burden was determined by limiting-dilution assay (39). At day 3 postinfection, after the completion of amastigote differentiation, both virulent GFPK10 and attenuated GFPK7 showed equal amounts of about 10^4 parasites per infected footpad (Fig. 3C), while the parasite burden of GFPK7 was more than 70-fold reduced at day 23 postinfection. These data confirm that GFPK7 virulence attenuation is not the result of increased susceptibility to host cytolytic activities but rather arises from a growth defect at the intracellular stage.

Expression of active GFP-LmaMPK7 inhibits amastigote growth in vitro. We further corroborated the amastigote growth defect utilizing previously established *L. donovani* GFP-LmaMPK transgenic parasites (LdGFPK), which showed GFP-LmaMPK7 phosphorylation and activity profiles identical to those of transgenic *L. major* GFPK7 (22). Unlike *L. major*, *L. donovani* allows for axenic amastigote differentiation (1, 17) and thus enabled us to study the growth phenotype in the absence of potential cytolytic host activities. A total of 5×10^5 promastigotes from a logarithmic culture were inoculated into fresh medium, and growth was assessed microscopically

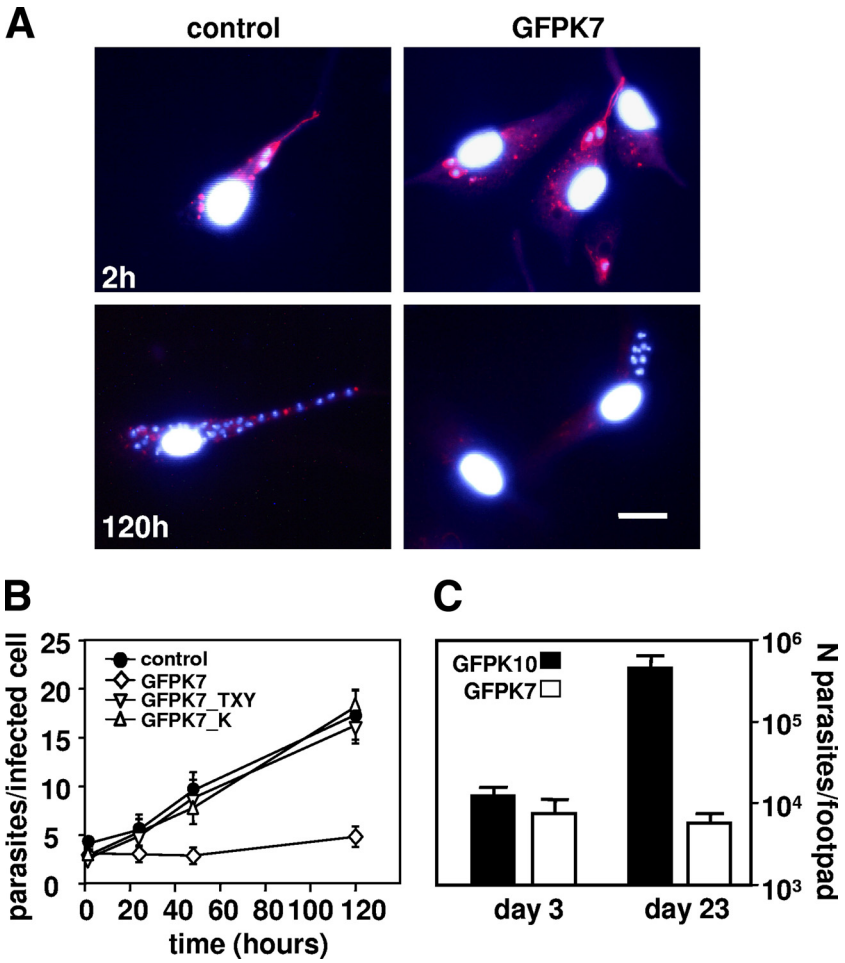

FIG. 3. Analysis of *L. major* GFPK7 amastigote differentiation and intracellular survival. (A) Immunofluorescence analysis. LPG was revealed at 2 h and 120 h postinfection in paraformaldehyde-fixed and ethanol (EtOH)-permeabilized cells by indirect immunofluorescence using monoclonal anti-phosphoglycan antibody WIC79.3 and Texas Red-conjugated anti-mouse IgG. Nuclei were counterstained with Hoechst 33341 dye. The bar corresponds to 20 μm. (B) Macrophage infection assay. PEMs were incubated for 2 h at 34°C with mock-transfected control (●) and transgenic GFPK7 (◇), GFPK7_TXY (▽), and GFPK7_K (△) metacyclic parasites at a multiplicity of 10 parasites per host cell, and free parasites were removed by washing with DMEM without serum. The numbers of intracellular parasites at 2 h and at days 1, 2, and 5 postinfection were estimated by nuclear staining with Hoechst 33341 dye and fluorescence microscopy. The bars indicate standard deviations for one representative triplicate experiment out of three independent experiments performed. (C) Limiting-dilution assay. Groups of 5 BALB/c mice were infected by footpad injection with 5×10^5 metacyclic parasites obtained from GFPK10 and GFPK7 stationary cultures, and parasite burden was determined at day 3 and day 23 postinfection by limiting dilution. The averages and standard deviations of triplicate determinations are shown.

by cell counting using a hemocytometer. The mock control and LdGFPK7 showed no difference in promastigote growth and reached stationary phase 5 days after inoculation (Fig. 4A, top). A total of 5×10^5 promastigotes from day 1 of stationary growth were reinoculated in low-pH medium and cultured at 37°C to induce the differentiation of axenic amastigotes. The control and LdGFPK7 developed amastigotes with the same efficiency; however, only control amastigotes showed normal proliferation and reached stationary growth 5 days later at a density of 6×10^7 cells/ml. In contrast, LdGFPK7 amastigotes stopped proliferating after only 2 days and reached a maximum density of 10^6 cells/ml, more than 50 times lower than the maximum density of the control (Fig. 4A, top). This growth defect was the result of increased LmaMPK7 activity, as both the GFPK7_TXY and GFPK7_K kinase-dead mutants showed normal amastigote proliferation (Fig. 4A, middle). The GFPK7 growth defect was reproduced by transgenic parasites expressing untagged LmaMPK7 and thus is independent from GFP expression (Fig. 4A, bottom). The growth arrest of GFPK7 was reversible, as the respective axenic amastigotes converted spontaneously into promastigotes at pH 7.4 and at 26°C (Fig. 4B). We routinely observed that GFPK7 converted into proliferating promastigotes faster than the mock control or GFPK10, a phenomenon that is documented by the substantial reduction in the generation time from 20 h in the control to 12 h in GFPK7 at 24 h after parasite conversion (Fig. 4C). These data suggest that LmaMPK7 may promote promastigote differentiation and firmly document the amastigote growth defect in LdGFPK7 in vitro.

LdGFPK7 shows a MAPK-dependent defect in proliferation and de novo protein biosynthesis. We used FACS-based approaches to further investigate the amastigote growth defect.

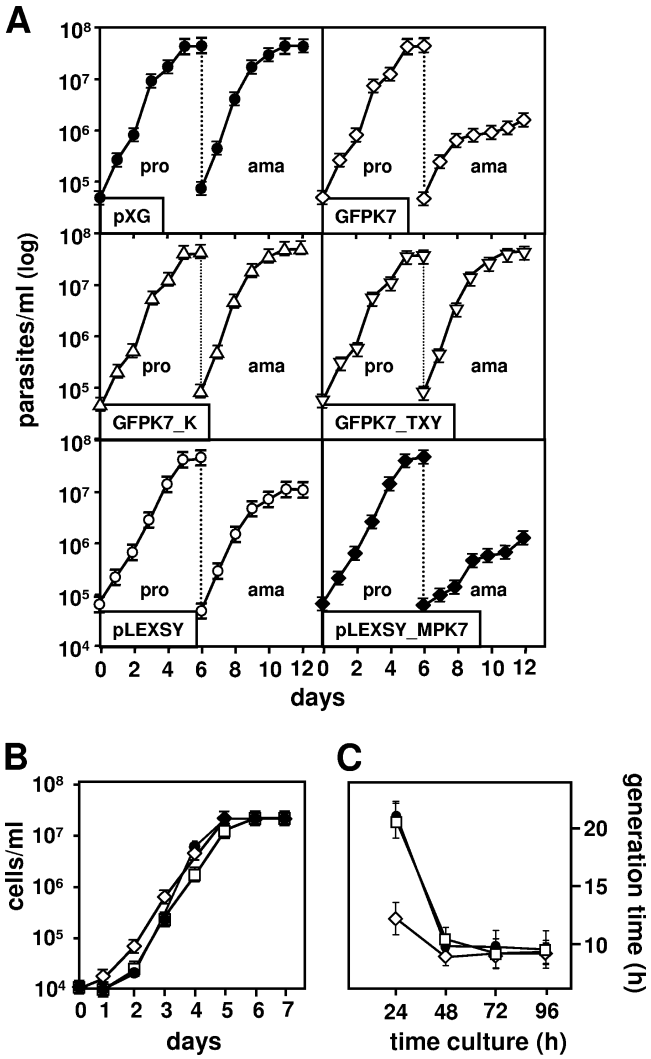

FIG. 4. LdGFPK7 axenic amastigotes show a severe growth defect. (A) Growth curve of axenic amastigotes. Growth of *L. donovani* pXG (●)- and pLEXSY (○)-transfected control and transgenic LdGFPK7 (◇), LdGFPK7_TXY (▽), LdGFPK7_K (△), and pLEXSY-LmaMPK7 (◆) promastigotes (pro) and axenic amastigotes (ama) was assessed microscopically by cell counting. The averages and standard deviations for triplicate determinations are shown. The data are representative of two independent experiments. (B and C) Determination of generation time. Logarithmically growing *L. donovani* axenic amastigotes of mock-transfected control (●) and transgenic LdGFPK7 (◇) and LdGFPK10 (□) cells were inoculated into promastigote culture medium at pH 7.4 and at 26°C, and growth was determined microscopically by cell counting (B). The generation time (C) was calculated based on the number of generations (n) during logarithmic growth using the formula $n = (\log_b - \log_B)/\log_2$, with b being the number of cells at the end of a 24-h time interval and B being the number of cells at the beginning of the 24-h time interval.

By utilizing a propidium iodide (PI) exclusion assay and flow cytometry, we identified a transient increase in levels of parasite death 24 h after the pH and temperature shift in both the control and LdGFPK7 (Fig. 5A). As the microscopic evaluation of LdGFPK7 growth did not account for parasite viability, we utilized an alternative, FACS-based proliferation assay, which allowed us to eliminate PI-positive dead parasites by cell gating (20). In this assay, the parasite cytoplasm is labeled with the fluorescent ester CFSE and cell growth is measured based on the fluorescence reduction of the daughter cells, which each inherit approximately half of the label. Control and LdGFPK7 promastigotes from the logarithmic phase were incubated with CFSE for 10 min in M199 medium at 26°C, unincorporated label was removed by centrifugation, and parasites were inoculated in amastigote medium. CFSE intensities were determined by flow cytometry 2 h and 72 h after labeling (Fig. 5B). After 72 h, the CFSE intensity in LdGFPK7 amastigotes showed a significantly higher fluorescence intensity than control cells, thus demonstrating a substantial reduction in proliferation. The contribution of GFP to the intense CFSE fluorescence was negligible as determined by analyzing unlabeled cells (Fig. 5B).

Increased LmaMPK7 activity may directly interfere with cell cycle regulation, leading to G_1/G_0 or G_2 arrest. We performed cell cycle analysis to test this possibility. The nuclear DNA content of control and transgenic LdGFPK7 parasites was measured at various time points during the promastigote-to-amastigote conversion. LdGFPK7 promastigotes showed normal cell cycle distribution, with 23% of cells in S phase, compared to 21% in mock-transfected controls (Fig. 5C). Both lines underwent synchronous cell cycle arrest in G_1/G_0 phase 6 h after culture in amastigote medium at a low pH and high temperature, an important checkpoint of amastigote differentiation previously described by Barak et al. (1). Control and LdGFPK7 cells efficiently reentered the cell cycle thereafter, as shown by the increase of S-phase cells to 27 to 29%. Despite the defect in proliferation, no significant difference in cell cycle distribution was observed for LdGFPK7 cells, indicating nonsynchronous growth arrest.

These data favor a model in which LdGFPK7 amastigote growth inhibition may result from a limitation in cellular metabolism rather than a specific effect on cell cycle regulation. We tested this hypothesis by determining the de novo protein biosynthesis in *L. donovani* mock transfectants and GFPK7 cells by metabolic labeling at various time points during the promastigote-to-amastigote conversion. Parasite growth in both lines was inhibited during the first 12 h and resumed in the control at 24 h after the induction of differentiation (Fig. 6A, left). Significantly, the proliferation rate correlated with biosynthetic activity, which was strongly reduced for the first 12 h but resumed at 24 h and reached normal levels at 48 h, when axenic amastigote differentiation is largely completed (Fig. 6A, right). In contrast, LdGFPK7 parasites showed a significant limitation of protein biosynthesis at 24 h, which remained at twofold-lower levels thereafter than the control. Western blot analysis of the abundance of the translation initiation factor eIF2α in total and phosphoprotein extracts correlated the reduction in de novo protein synthesis at 24 h in LdGFPK7 cells with increased levels of eIF2α phosphorylation and, thus, the inactive form of this factor (Fig. 6B). Together, these data support a model where the inhibition of LdGFPK7 amastigote proliferation may be the result of limitations in biosynthetic activity, which may then lead to the nonsynchronous cell cycle arrest characteristic of stationary-phase cells.

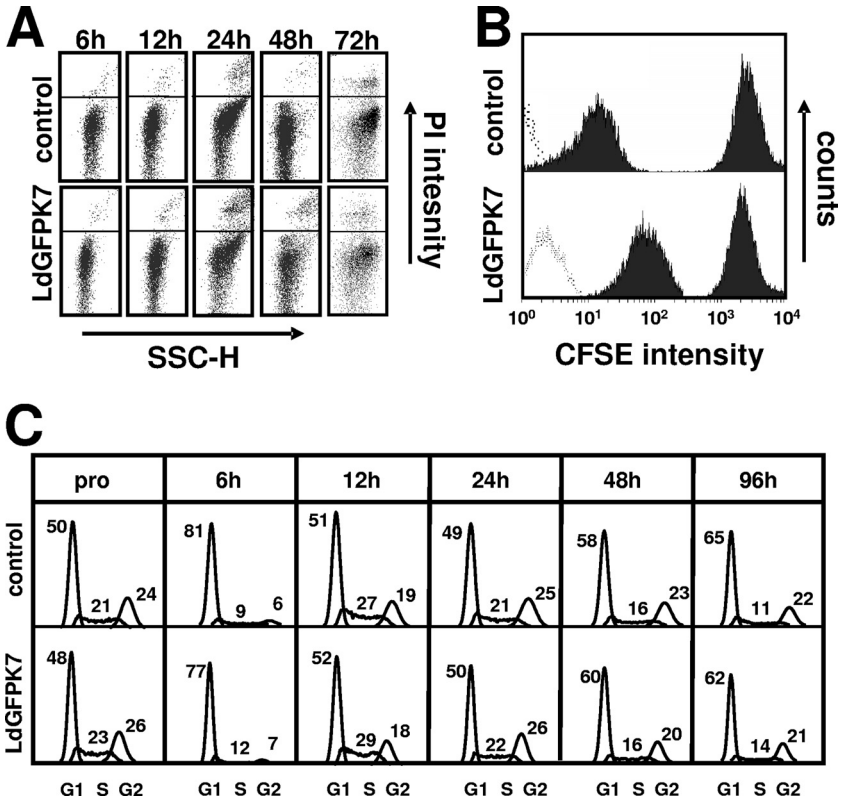

FIG. 5. The *L. donovani* GFPK7 growth defect is independent from cell death and cell cycle arrest. (A) FACS analysis. Control and LdGFPK7 promastigotes were inoculated into amastigote medium, and the number of propidium iodide-positive dead cells was determined during the promastigote-to-amastigote conversion at the indicated time points by flow cytometry. The *x* axis represents cell size (sideward scatter [SSC-H]), and the *y* axis shows propidium iodide fluorescence intensity determined by using the FL2-H channel. Representative profiles of one triplicate experiment are shown. (B) Proliferation assay. FACS analysis was performed on CFSE-stained control and LdGFPK7 amastigotes 2 h and 72 h after labeling. FACS profiles are representative of three independent experiments. The dotted lines represent unstained cells. The experiment was gated on PI-negative cells. (C) Cell cycle analysis. The nuclear DNA content of control and LdGFPK7 cells from logarithmic promastigote cultures (pro) and at various time points after inoculation into amastigote medium was determined by propidium iodide staining and FACS analysis. Cells with the DNA content 2n/4n were gated on fluorescence FL2 pulse-versus-area measurements to exclude cell doublets from the analysis. The percentage of cells in different cell cycle phases was calculated by using the Watson pragmatic model of FlowJo (v6.1) software.

DISCUSSION

Leishmania undergoes various adaptive differentiation steps during the infectious cycle that are coupled to growth control. At a high density in culture or inside the sand fly midgut, proliferating procyclic promastigotes differentiate into nondividing, highly virulent metacyclic parasites. These parasites reenter the cell cycle after differentiation into the intracellular amastigote form, which proliferates inside host macrophages and establishes the acute phase of *Leishmania* infection. The different developmental transitions are accompanied by changes in phosphoprotein abundance and the overall phosphorylation pattern (11, 23, 24), suggesting a crucial role for protein kinases and phosphatases in parasite development and pathogenicity. We previously provided evidence for an environmentally induced and amastigote-specific activity of three *Leishmania* MAPKs utilizing transgenic parasites expressing GFP-LmaMPK fusion proteins (22). Here, by utilizing GFPK-LmaMPK7 transgenic lines expressing functional or inactive kinase, we established a first link of LmaMPK7 phosphotransferase activity to *Leishmania* growth control and de novo protein biosynthesis. Our data allow new insight into LmaMPK7 biology, which escapes classical biochemical and gene-targeting approaches due to the low expression levels of this protein and the generation of a lethal null mutant phenotype (Morales et al., unpublished).

GFPK7 transgenic parasites expressing the functional GFP-LmaMPK7 fusion protein were strongly compromised in their ability to elicit cutaneous lesions in mouse footpad experiments (Fig. 1). We showed that this defect was independent from host cytolytic activities (Fig. 2) or defects in parasite differentiation (Fig. 3) but linked to a defect in amastigote proliferation (Fig. 4A and 5B).

The GFPK7 proliferation defect is reminiscent of the growth phenotypes of a number of MAPK mutants in other trypanosomatids. The inactivation of the *L. mexicana* MAPK LMPK (now referred to as LmxMPK1 [44]) abrogated amastigote growth without an effect on differentiation or promastigote proliferation (43). In *Trypanosoma brucei*, null mutants of TbMAPK2 showed a delay in procyclic differentiation, aberrations in cellular and nuclear morphology, and a defect in cell proliferation at this stage (25). Likewise, the deletion of TbMAPK5 or the overexpression of a kinase-dead mutant of

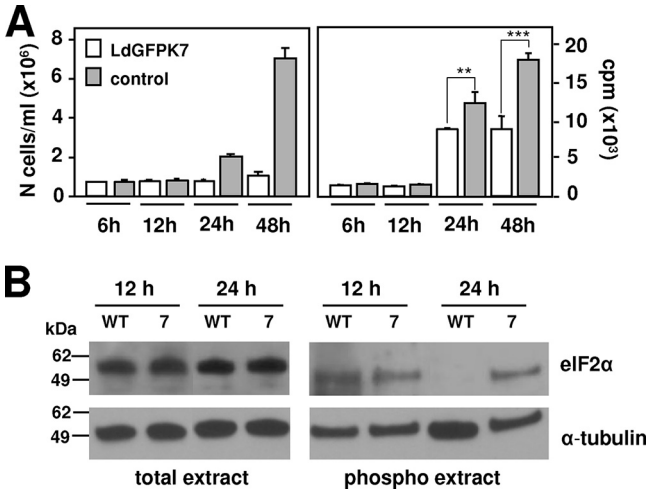

FIG. 6. The *L. donovani* GFPK7 growth defect is linked to limited de novo protein biosynthesis. (A) Metabolic labeling. (Left) Control and LdGFPK7 promastigotes were inoculated into amastigote medium, and the number of parasites was determined microscopically by cell counting. (Right) De novo protein biosynthesis was assessed at the time points indicated by metabolic labeling with Pro-Mix containing L-[^{35}S]methionine and L-[^{35}S]cysteine (GE Healthcare). Protein amounts were normalized by equal cell numbers. An unpaired *t* test was applied to the 24- and 48-h time points. **, *P* value of 0.0018; ***, *P* value of 0.0001. (B) Western blotting. Total protein extracts or purified phosphoproteins obtained from wild-type (WT) or GFPK7 (7) parasites 12 h and 24 h after the induction of amastigote differentiation were separated by SDS-PAGE, and the abundance of eIF2α was revealed by Western blotting. The levels of α-tubulin expression were assessed for normalization purposes. Molecular mass standards are indicated (in kilodaltons).

this protein was associated with premature parasite differentiation into the nonproliferating stumpy bloodstream form (14). The MAPK-related *T. brucei* kinase TbECK1 was previously linked to growth control utilizing transgenic parasites expressing a C-terminal deletion mutant of this protein kinase (16). These data, together with our own findings, clearly establish an important link of the trypanosomatid MAPK pathway in parasite growth control and virulence.

Our data provide the first evidence for a function of LmaMPK7 in the control of *Leishmania* proliferation, which may occur through a direct regulatory role in the cell cycle machinery. Mammalian MAPKs control cell cycle progression by activating cyclin D1-cdk4 or cyclin B-CDC2 complexes (4, 46). Studies of fibroblast cultures have shown that MAPKs exert both positive and negative effects on cellular growth depending on the level and duration of kinase activity. Transfection experiments using active MKK Raf-1 correlated low MAPK activity with growth stimulation and high MAPK activity with cell cycle arrest (33), a phenomenon due to the differential expression of cell cycle-promoting cyclin D1 and cyclin-dependent kinase inhibitor p21^{cip}, respectively (26, 45). Although we cannot rule out a similar scenario for GFPK7 amastigotes, a nonsynchronous inhibition of cell growth is more consistent with a broader metabolic deficiency rather than a cell cycle-specific defect. This possibility is further supported by our observation that GFPK7 amastigotes show a substantial reduction of de novo protein biosynthesis (Fig. 6A). Increased LmaMPK7 phosphotransferase activity correlated with prolonged eIF2α phosphorylation following the promastigote-to-amastigote conversion (Fig. 6B), which may interfere with translation initiation and subsequently cause the various downstream effects, including growth inhibition.

There are three possible scenarios for how the overexpression of active LmaMPK7 may limit the rate of protein translation. First, transgenic LmaMPK7 may be recognized in an inappropriate way by a higher-order MAPK kinase (MKK) and thus interfere with the phosphorylation of a downstream MAPK that positively regulates protein translation. However, we would expect that such a quenching effect should also occur by the overexpression of the inactive LmaMPK7 mutant in GFPK7_K, which retains its normal TXY activation loop but is unable to catalyze substrate phosphorylation (22). The absence of any virulence or growth defect in these cells thus rules out this quenching model (Fig. 1C, 3B, and 4A).

Second, it is possible that increased LmaMPK7 activity leads to a nonspecific phosphorylation of unphysiological substrates, with a broad effect on cellular metabolism, including protein translation. Although we cannot rule out this possibility, the reversibility of the growth defect of GFPK7 amastigotes (Fig. 4B) and the absence of any significant effects on the viability of these cells (Fig. 5A) are rather uncharacteristic for such a pleiotropic and nonspecific phenotype. Furthermore, the overexpression of related LmaMPK10 had no effect on parasite virulence (Fig. 1) despite its coinduction during amastigote differentiation (22).

We favor a third model, in which increased LmaMPK7 activity leads to the overphosphorylation of its endogenous substrates, which may be implicated in the regulation of protein translation. Protein phosphorylation plays a crucial role in regulating translation initiation with both stimulatory and inhibitory effects on protein synthesis. Translation initiation is enhanced, for example, by the phosphorylation of the translation initiation factor eIF4E on Ser209 following the treatment of cells with growth factors and mitogens through the MAPK-activated protein kinase Mnk1 (28). In contrast, as part of the cellular response to environmental stress, inhibition of translation occurs through the phosphorylation of the α subunit of eIF2 at Ser51 by specific eIF2 kinases (13). Hence, based on our previously reported findings that LmaMPK7 activity is enhanced in response to heat and pH shock (22) and the prolonged phosphorylation of eIF2α in GFPK7, it is possible that increased LmaMPK7 activity mimics an intracellular stress response, which may affect the regulatory networks underlying translation initiation. Our current efforts focus on the identification of these signaling networks by quantitative phosphoproteomics and the identification of endogenous phosphoprotein substrates that are overphosphorylated in GFPK7. The elucidation of parasite molecules that underlie the growth phenotype of GFPK7 amastigotes in intracellular proliferation will hence increase our understanding of *Leishmania* growth control and translational regulation, with potential applicability to antimicrobial interventions.

ACKNOWLEDGMENTS

This work was supported by the INSERM Avenir Program and the Institut Pasteur Bourse Roux (M.A.M.).

We thank Dan Zilberstein, Technion, Israel, for providing the anti-eIF2α antibody.

REFERENCES

1. **Barak, E., S. Amin-Spector, E. Gerliak, S. Goyard, N. Holland, and D. Zilberstein.** 2005. Differentiation of Leishmania donovani in host-free system: analysis of signal perception and response. Mol. Biochem. Parasitol. **141:**99–108.
2. **Brook, M., G. Sully, A. R. Clark, and J. Saklatvala.** 2000. Regulation of tumour necrosis factor alpha mRNA stability by the mitogen-activated protein kinase p38 signalling cascade. FEBS Lett. **483:**57–61.
3. **Chappuis, F., S. Sundar, A. Hailu, H. Ghalib, S. Rijal, R. W. Peeling, J. Alvar, and M. Boelaert.** 2007. Visceral leishmaniasis: what are the needs for diagnosis, treatment and control? Nat. Rev. Microbiol. **5:**873–882.
4. **Cheng, M., V. Sexl, C. J. Sherr, and M. F. Roussel.** 1998. Assembly of cyclin D-dependent kinase and titration of p27Kip1 regulated by mitogen-activated protein kinase kinase (MEK1). Proc. Natl. Acad. Sci. U. S. A. **95:**1091–1096.
5. **Clayton, C., and M. Shapira.** 2007. Post-transcriptional regulation of gene expression in trypanosomes and leishmanias. Mol. Biochem. Parasitol. **156:** 93–101.
6. **Clayton, C. E.** 2002. Life without transcriptional control? From fly to man and back again. EMBO J. **21:**1881–1888.
7. **da Silva, R., and D. L. Sacks.** 1987. Metacyclogenesis is a major determinant of Leishmania promastigote virulence and attenuation. Infect. Immun. **55:** 2802–2806.
8. **Davis, R. J.** 1995. Transcriptional regulation by MAP kinases. Mol. Reprod. Dev. **42:**459–467.
9. **Dean, J. L., M. Brook, A. R. Clark, and J. Saklatvala.** 1999. p38 mitogen-activated protein kinase regulates cyclooxygenase-2 mRNA stability and transcription in lipopolysaccharide-treated human monocytes. J. Biol. Chem. **274:**264–269.
10. **Debrabant, A., M. B. Joshi, P. F. Pimenta, and D. M. Dwyer.** 2004. Generation of Leishmania donovani axenic amastigotes: their growth and biological characteristics. Int. J. Parasitol. **34:**205–217.
11. **Dell, K. R., and J. N. Engel.** 1994. Stage-specific regulation of protein phosphorylation in Leishmania major. Mol. Biochem. Parasitol. **64:**283–292.
12. **Desjeux, P.** 2004. Leishmaniasis: current situation and new perspectives. Comp. Immunol. Microbiol. Infect. Dis. **27:**305–318.
13. **Dever, T. E.** 2002. Gene-specific regulation by general translation factors. Cell **108:**545–556.
14. **Domenicali Pfister, D., G. Burkard, S. Morand, C. K. Renggli, I. Roditi, and E. Vassella.** 2006. A mitogen-activated protein kinase controls differentiation of bloodstream forms of Trypanosoma brucei. Eukaryot. Cell **5:**1126–1135.
15. **Dwyer, D. M.** 1976. Antibody-induced modulation of Leishmania donovani surface membrane antigens. J. Immunol. **117:**2081–2091.
16. **Ellis, J., M. Sarkar, E. Hendriks, and K. Matthews.** 2004. A novel ERK-like, CRK-like protein kinase that modulates growth in Trypanosoma brucei via an autoregulatory C-terminal extension. Mol. Microbiol. **53:**1487–1499.
17. **Goyard, S., H. Segawa, J. Gordon, M. Showalter, R. Duncan, S. J. Turco, and S. M. Beverley.** 2003. An in vitro system for developmental and genetic studies of Leishmania donovani phosphoglycans. Mol. Biochem. Parasitol. **130:**31–42.
18. **Hunter, T.** 1998. The role of tyrosine phosphorylation in cell growth and disease. Harvey Lect. **94:**81–119.
19. **Ivens, A. C., C. S. Peacock, E. A. Worthey, L. Murphy, G. Aggarwal, M. Berriman, E. Sisk, M. A. Rajandream, E. Adlem, R. Aert, A. Anupama, Z. Apostolou, P. Attipoe, N. Bason, C. Bauser, A. Beck, S. M. Beverley, G. Bianchettin, K. Borzym, G. Bothe, C. V. Bruschi, M. Collins, E. Cadag, L. Ciarloni, C. Clayton, R. M. Coulson, A. Cronin, A. K. Cruz, R. M. Davies, J. De Gaudenzi, D. E. Dobson, A. Duesterhoeft, G. Fazelina, N. Fosker, A. C. Frasch, A. Fraser, M. Fuchs, C. Gabel, A. Goble, A. Goffeau, D. Harris, C. Hertz-Fowler, H. Hilbert, D. Horn, Y. Huang, S. Klages, A. Knights, M. Kube, N. Larke, L. Litvin, A. Lord, T. Louie, M. Marra, D. Masuy, K. Matthews, S. Michaeli, J. C. Mottram, S. Muller-Auer, H. Munden, S. Nelson, H. Norbertczak, K. Oliver, S. O'Neil, M. Pentony, T. M. Pohl, C. Price, B. Purnelle, M. A. Quail, E. Rabbinowitsch, R. Reinhardt, M. Rieger, J. Rinta, J. Robben, L. Robertson, J. C. Ruiz, S. Rutter, D. Saunders, M. Schafer, J. Schein, D. C. Schwartz, K. Seeger, A. Seyler, S. Sharp, H. Shin, D. Sivam, R. Squares, S. Squares, V. Tosato, C. Vogt, G. Volckaert, R. Wambutt, T. Warren, H. Wedler, J. Woodward, S. Zhou, W. Zimmermann, D. F. Smith, J. M. Blackwell, K. D. Stuart, B. Barrell, and P. J. Myler.** 2005. The genome of the kinetoplastid parasite, Leishmania major. Science **309:** 436–442.
20. **Kamau, S. W., M. Hurtado, U. U. Muller-Doblies, F. Grimm, and R. Nunez.** 2000. Flow cytometric assessment of allopurinol susceptibility in Leishmania infantum promastigote. Cytometry **40:**353–360.
21. **Kapler, G. M., C. M. Coburn, and S. M. Beverley.** 1990. Stable transfection of the human parasite Leishmania major delineates a 30-kilobase region sufficient for extrachromosomal replication and expression. Mol. Cell. Biol. **10:**1084–1094.
22. **Morales, M. A., O. Renaud, W. Faigle, S. L. Shorte, and G. F. Spath.** 2007. Over-expression of Leishmania major MAP kinases reveals stage-specific induction of phosphotransferase activity. Int. J. Parasitol. **37:**1187–1199.
23. **Morales, M. A., R. Watanabe, C. Laurent, P. Lenormand, J. C. Rousselle, A. Namane, and G. F. Spath.** 2008. Phosphoproteomic analysis of Leishmania donovani pro- and amastigote stages. Proteomics **8:**350–363.
24. **Mukhopadhyay, N. K., A. K. Saha, J. K. Lovelace, R. Da Silva, D. L. Sacks, and R. H. Glew.** 1988. Comparison of the protein kinase and acid phosphatase activities of five species of Leishmania. J. Protozool. **35:**601–607.
25. **Muller, I. B., D. Domenicali-Pfister, I. Roditi, and E. Vassella.** 2002. Stage-specific requirement of a mitogen-activated protein kinase by Trypanosoma brucei. Mol. Biol. Cell **13:**3787–3799.
26. **Parry, D., D. Mahony, K. Wills, and E. Lees.** 1999. Cyclin D-CDK subunit arrangement is dependent on the availability of competing INK4 and p21 class inhibitors. Mol. Cell. Biol. **19:**1775–1783.
27. **Parsons, M., E. A. Worthey, P. N. Ward, and J. C. Mottram.** 2005. Comparative analysis of the kinomes of three pathogenic trypanosomatids: Leishmania major, Trypanosoma brucei and Trypanosoma cruzi. BMC Genomics **6:**127.
28. **Pyronnet, S., H. Imataka, A. C. Gingras, R. Fukunaga, T. Hunter, and N. Sonenberg.** 1999. Human eukaryotic translation initiation factor 4G (eIF4G) recruits mnk1 to phosphorylate eIF4E. EMBO J. **18:**270–279.
29. **Rotureau, B., M. A. Morales, P. Bastin, and G. F. Spath.** 2009. The flagellum-MAP kinase connection in trypanosomatids: a key sensory role in parasite signaling and development? Cell. Microbiol. **11:**710–718.
30. **Saar, Y., A. Ransford, E. Waldman, S. Mazareb, S. Amin-Spector, J. Plumblee, S. J. Turco, and D. Zilberstein.** 1998. Characterization of developmentally-regulated activities in axenic amastigotes of Leishmania donovani. Mol. Biochem. Parasitol. **95:**9–20.
31. Reference deleted.
32. **Sacks, D. L., and P. V. Perkins.** 1984. Identification of an infective stage of Leishmania promastigotes. Science **223:**1417–1419.
33. **Sewing, A., B. Wiseman, A. C. Lloyd, and H. Land.** 1997. High-intensity Raf signal causes cell cycle arrest mediated by p21Cip1. Mol. Cell. Biol. **17:**5588–5597.
34. **Spath, G. F., and S. M. Beverley.** 2001. A lipophosphoglycan-independent method for isolation of infective Leishmania metacyclic promastigotes by density gradient centrifugation. Exp. Parasitol. **99:**97–103.
35. **Spath, G. F., L. Epstein, B. Leader, S. M. Singer, H. A. Avila, S. J. Turco, and S. M. Beverley.** 2000. Lipophosphoglycan is a virulence factor distinct from related glycoconjugates in the protozoan parasite Leishmania major. Proc. Natl. Acad. Sci. U. S. A. **97:**9258–9263.
36. **Spath, G. F., L. A. Garraway, S. J. Turco, and S. M. Beverley.** 2003. The role(s) of lipophosphoglycan (LPG) in the establishment of Leishmania major infections in mammalian hosts. Proc. Natl. Acad. Sci. U. S. A. **100:** 9536–9541.
37. **Spath, G. F., L. F. Lye, H. Segawa, D. L. Sacks, S. J. Turco, and S. M. Beverley.** 2003. Persistence without pathology in phosphoglycan-deficient Leishmania major. Science **301:**1241–1243.
38. **Titus, R. G., F. J. Gueiros-Filho, L. A. de Freitas, and S. M. Beverley.** 1995. Development of a safe live Leishmania vaccine line by gene replacement. Proc. Natl. Acad. Sci. U. S. A. **92:**10267–10271.
39. **Titus, R. G., M. Marchand, T. Boon, and J. A. Louis.** 1985. A limiting dilution assay for quantifying Leishmania major in tissues of infected mice. Parasite Immunol. **7:**545–555.
40. **Titus, R. G., I. Muller, P. Kimsey, A. Cerny, R. Behin, R. M. Zinkernagel, and J. A. Louis.** 1991. Exacerbation of experimental murine cutaneous leishmaniasis with CD4+ Leishmania major-specific T cell lines or clones which secrete interferon-gamma and mediate parasite-specific delayed-type hypersensitivity. Eur. J. Immunol. **21:**559–567.
41. **Tolson, D. L., S. J. Turco, and T. W. Pearson.** 1990. Expression of a repeating phosphorylated disaccharide lipophosphoglycan epitope on the surface of macrophages infected with Leishmania donovani. Infect. Immun. **58:**3500–3507.
42. **Wang, Q., I. M. Melzer, M. Kruse, C. Sander-Juelch, and M. Wiese.** 2005. LmxMPK4, a mitogen-activated protein (MAP) kinase homologue essential for promastigotes and amastigotes of Leishmania mexicana. Kinetoplastid Biol. Dis. **4:**6.
43. **Wiese, M.** 1998. A mitogen-activated protein (MAP) kinase homologue of Leishmania mexicana is essential for parasite survival in the infected host. EMBO J. **17:**2619–2628.
44. **Wiese, M.** 2007. Leishmania MAP kinases—familiar proteins in an unusual context. Int. J. Parasitol. **37:**1053–1062.
45. **Woods, D., D. Parry, H. Cherwinski, E. Bosch, E. Lees, and M. McMahon.** 1997. Raf-induced proliferation or cell cycle arrest is determined by the level of Raf activity with arrest mediated by p21Cip1. Mol. Cell. Biol. **17:**5598–5611.
46. **Wright, J. H., E. Munar, D. R. Jameson, P. R. Andreassen, R. L. Margolis, R. Seger, and E. G. Krebs.** 1999. Mitogen-activated protein kinase kinase activity is required for the G(2)/M transition of the cell cycle in mammalian fibroblasts. Proc. Natl. Acad. Sci. U. S. A. **96:**11335–11340.
47. **Zilberstein, D., and M. Shapira.** 1994. The role of pH and temperature in the development of Leishmania parasites. Annu. Rev. Microbiol. **48:**449–470.